Molecular Structures of Pentamethylarsenic(V) and Trimethyldichloroarsenic(V) by Gas Electron Diffraction and ab Initio Calculations: Molecular Mechanics Calculations on Pentamethylarsenic(V), Pentaphenylarsenic(V), and Related Compounds

Tim M. Greene,*,† Anthony J. Downs,† Colin R. Pulham,‡ Arne Haaland,*,§ Hans Peter Verne,§ Hans Vidar Volden,§ and Tatjana V. Timofeeva*,¶

Department of Chemistry, University of Oxford, South Parks Road, Oxford, OX1 3QR, U.K., Department of Chemistry, The University of Edinburgh, West Mains Road, Edinburgh, EH9 3JJ, Scotland, U.K., Department of Chemistry, University of Oslo, PO Box 1033 Blindern, N-0315 Oslo, Norway, and Institute of Organoelement Compounds, Russian Academy of Sciences, Vavilov Street 28, Moscow 117813, Russia

Received June 22, 1998

The molecular structures of $AsMe_5$ and $AsMe_3Cl_2$ (Me = CH_3) have been determined by gas electron diffraction and Hartree−Fock computations. Both molecules are found to have trigonal bipyramidal arrangements of the heavy atom skeleton. The bond distances (r_a) for $AsMe_5$ are As−C_{eq} = 197.5(3) pm and As−C_{ax} = 207.3(4) pm; for $AsMe_3Cl_2$, As−C_{eq} = 192.5-(2) pm and As−Cl_{ax} = 234.9(3) pm. The coordination geometries and dimensions are compared with those of related molecules. Molecular mechanics calculations on the pentamethyl and pentaphenyl derivatives of P, As, Sb, and Bi reproduce the observed coordination geometries and indicate that the square pyramidal equilibrium structures of $SbPh_5$ and $BiPh_5$ are stabilized by Coulombic interactions between the ligands.

1. Introduction

Two symmetrical coordination geometries are possible for pentavalent compounds of the heavier group 15 elements P, As, Sb, or Bi, viz., the trigonal bipyramid (TBP) and the square pyramid (SP), as depicted in Figure 1. The valence shell electron-pair repulsion (VSEPR) model[1] is generally held to favor the TBP over the SP. This is based upon the simple assumption that the gross repulsion between electron pairs is smaller in the TBP with six valence angles of 90° than in the SP with eight such angles (or alternatively four angles somewhat smaller than 90° and four somewhat larger).

The TBP arrangement is indeed found for pentamethylantimony(V), $SbMe_5$, until now the only pentaorgano compound of the heavier group 15 elements to have had its structure determined in the gaseous state.[2,3] The structure of $SbMe_5$ in the liquid phase, inferred from its vibrational spectrum,[4] and in the solid state, as determined by X-ray crystallography,[5] are in accord with that adopted by the gaseous molecule. Ab initio molecular orbital calculations on $SbMe_5$, with an effective core potential (ECP) and a DZ basis for the valence shell of the metal atom and with electron correlation treated by the modified coupled pair functional (MCPF) method, indicate that the energy of the optimal SP model lies 7.1 kJ mol^{-1} above the ground state.[3]

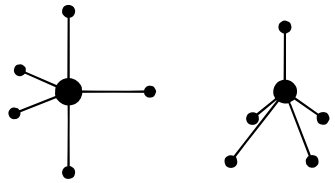

Figure 1. The trigonal bipyramid (TBP) and the square pyramid (SP).

The bismuth compound $BiMe_5$, recently synthesized by Wallenhauer and Seppelt, has been shown to adopt a TBP structure in the crystalline phase.[6] We have attempted to record the gas electron diffraction (GED) pattern with an all-glass inlet system at room temperature, but found that the sample decomposed to yield $BiMe_3$.[7] Ab initio calculations at the ECP/MCFP level indicate that the energy of the SP configuration relative to the TBP is higher than in the Sb analogue, viz., ΔE = 10.5 kJ mol^{-1}.[3]

* To whom correspondence should be addressed.
† University of Oxford.
‡ The University of Edinburgh.
§ University of Oslo.
¶ Institute of Organoelement Compounds, Russian Academy of Sciences.

(1) Gillespie, R. J.; Nyholm, R. S. *Q. Rev. Chem. Soc.* **1957**, *11*, 339. Gillespie, R. J. *Molecular Geometry*; Van Nostrand Reinhold: London, 1972. Gillespie, R. J. *Chem. Soc. Rev.* **1992**, *21*, 59. Gillespie, R. J.; Hargittai, I. *The VSEPR Model of Molecular Geometry*; Allyn and Bacon: Boston, 1991.

(2) Pulham, C. R.; Haaland, A.; Hammel, A.; Rypdal, K.; Verne, H. P.; Volden, H. V. *Angew. Chem., Int. Ed. Engl.* **1992**, *31*, 1464.

(3) Haaland, A.; Hammel, A.; Rypdal, K.; Swang, O.; Brunvoll, J.; Gropen, O.; Greune, M.; Weidlein, J. *Acta Chem. Scand.* **1993**, *47*, 368.

(4) Downs, A. J.; Schmutzler, R.; Steer, I. A. *Chem. Commun.* **1966**, 221.

(5) Wallenhauer, S.; Seppelt, K. *Inorg. Chem.* **1995**, *34*, 116.

(6) Wallenhauer, S.; Seppelt, K. *Angew. Chem., Int. Ed. Engl.* **1994**, *33*, 976.

(7) Wallenhauer, S.; Seppelt, K.; Verne, H. P.; Volden, H. V. Unpublished results.

10.1021/om980520r CCC: $15.00
Publication on Web 10/29/1998

Investigations by single-crystal X-ray diffraction have shown that pentaphenylphosphorus(V), PPh_5, takes up a TBP structure in the solid phase,[8] and so presumably does $AsPh_5$ since crystals of the two compounds are isomorphous.[9] The structure of $AsPh_5$ cocrystallized with half a mole of cyclohexane per mole of $AsPh_5$ has also been shown to be TBP.[10]

It created quite a stir, therefore, when, about 35 years ago, crystalline pentaphenylantimony(V), $SbPh_5$, was shown to have a coordination geometry much closer to SP than to TBP.[11] Furthermore, comparison of the vibrational spectra (IR and Raman) of the solid As and Sb pentaphenyls with those of solutions in CH_2Cl_2 or CH_2Br_2 implies that the solid-state configurations, TBP and SP, respectively, are retained in solution.[12] When $SbPh_5$ is cocrystallized with half a mole of cyclohexane, $SbPh_5 \cdot {}^1/_2C_6H_{12}$, the structure is TBP,[13] as is that of the closely related compound penta-*p*-tolylantimony(V).[14] The energy difference between the SP and TBP configurations is obviously so small that it may be overcome by intermolecular forces in the crystal. Finally, Seppelt and co-workers have shown that $BiPh_5$, like the Sb analogue, is SP in the crystalline phase.[15]

All the pentamethyl and pentaaryl compounds discussed above are highly fluxional, and the organic ligands in each are equivalent on the NMR time scale. The exchange of axial and equatorial substituents in the TBP complexes presumably occurs via an SP transition state, while the exchange of apical and basal substituents in the SP complexes occurs via a TBP state. We are aware of only one case in which it has been possible to slow the process sufficiently by cooling to allow the relative energy of the less stable configuration to be determined by NMR measurements: the barrier to ligand exchange in penta-*p*-tolylantimony in $CHFCl_2$ is 6.7 and 6.1 kJ mol^{-1} by line-shape analysis of the ^1H and ^{13}C spectra, respectively.[16] The spectra did not, however, reveal which configuration, SP or TBP, has the lower energy. Since $SbPh_5$ is SP in halogenomethane solvents, one might assume this to be the case also for Sb(*p*-tolyl)$_5$ (in contrast to its crystalline structure), indicating that the energy for the TBP configuration is about 6.4 kJ mol^{-1} higher than that of the SP configuration.

The molecular configurations and the average E−C bond distances of the molecules discussed above are summarized in Table 1. Further discussions of the structures of pentacoordinate Bi and Sb compounds can be found elsewhere.[5] It is clear from these examples that there exists in the solid phase or in solution only a small energy separation between the two molecular geometries. To ascertain whether this is true also for the isolated molecules, substantially more structural studies of the gaseous molecules need to be undertaken. In this context, it may be noted that the transition-metal compound $TaMe_5$ has been shown to be SP in the gas phase, unlike its main group analogue $SbMe_5$.[2]

Table 1. Configurations and Average E−C Bond Lengths (in pm) for Some ER_5 Compounds (R = Organic Ligand; E = P, As, Sb, or Bi)

compound	config	$\langle r_{E-C} \rangle$	ref
$AsMe_5$	TBP	201	this work
$SbMe_5$	TBP	219	2
$BiMe_5$	TBP	228	6
PPh_5	TBP	191	8
$AsPh_5 \cdot {}^1/_2$hex[a]	TBP	202	10
Sb(^{p}tol)$_5$	TBP	219	14
$SbPh_5 \cdot {}^1/_2$hex[a]	TBP	218	13
$SbPh_5$	SP	220	11
$BiPh_5$	SP	230	15

[a] hex = cyclohexane.

In this paper we describe the findings of a gas electron diffraction (GED) study and Hartree−Fock (HF) ab initio calculations involving pentamethylarsenic[17] and its precursor trimethyldichloroarsenic. The structural properties deduced are compared with those of analogous molecules. Finally, we have carried out molecular mechanics calculations on the pentamethyl and pentaphenyl derivatives of P, As, Sb, and Bi in order to assess the effect of ligand−ligand interactions on the relative stabilities of the TBP and SP configurations.

2. Experimental Section

2.1. Synthesis. Trimethylarsine was synthesized by the reaction of CH_3Li (1.4 M solution in diethyl ether, Aldrich) with arsenic trichloride (BDH) and converted to $AsMe_3Cl_2$ by treatment with a solution of chlorine gas in carbon tetrachloride.[18] The compound was sublimed in vacuo, and its purity checked by reference to its ^1H NMR[19] and Raman spectra.[20] Reaction of $AsMe_3Cl_2$ with CH_3Li in dimethyl ether at −60 °C, following the procedure described by Mitschke and Schmidbaur,[17] yielded a sample of pentamethylarsenic(V). The product obtained was further purified by fractional condensation in vacuo, and the absence of significant levels of impurity checked by reference to its vibrational and ^1H NMR spectra.[17] The solution of CH_3Li in dimethyl ether was prepared by the reaction of Li metal (BDH) with CH_3Cl.

2.2. Electron Diffraction Measurements. The scattering patterns were recorded using a Balzers Eldigraph KDG-2 system[21] with electron wavelengths (determined by reference to the scattering pattern of benzene) of 5.866 pm ($AsMe_5$) and 5.846 pm ($AsMe_3Cl_2$). Photographic plates were exposed at nozzle-to-plate distances of ca. 25 and 50 cm, yielding data spanning the *s*-range 17.5−300.0 nm^{-1}. Standard scattering factors were used in the refinement.[22] Relevant details of the experimental conditions are given in Table 2.

For the $AsMe_5$ vapor an all-glass inlet system was used with the bulk of the compound kept outside the apparatus in a cooled container. The plates were traced at the "Snoopy" densitometer, and the results were processed by standard procedures.[23]

(8) Wheatley, P. J. *J. Chem. Soc.* **1964**, 2206.
(9) Wheatley, P. J.; Wittig, G. *Proc. Chem. Soc. London* **1962**, 251.
(10) Brock, C. P.; Webster, D. F. *Acta Crystallogr.* **1976**, *B32*, 2089.
(11) Wheatley, P. J. *J. Chem. Soc.* **1964**, 3718. Beauchamp, A. L.; Bennett, M. J.; Cotton, F. A. *J. Am. Chem. Soc.* **1968**, *90*, 6675.
(12) Kok, G. L. *Spectrochim. Acta* **1974**, *30A*, 961.
(13) Brabant, C.; Blanck, B.; Beauchamp, A. L. *J. Organomet. Chem.* **1974**, *82*, 231.
(14) Brabant, C.; Hubert, J.; Beauchamp, A. L. *Can. J. Chem.* **1973**, *51*, 2952.
(15) Schmuck, A.; Buschmann, J.; Fuchs, J.; Seppelt, K. *Angew. Chem., Int. Ed. Engl.* **1987**, *26*, 1180.
(16) Kuykendall, G. L.; Mills, J. L. *J. Organomet. Chem.* **1976**, *118*, 123.
(17) Mitschke, K.-H.; Schmidbaur, H. *Chem. Ber.* **1973**, *106*, 3645.
(18) Dyke, W. J. C.; Davies, G.; Jones, W. J. *J. Chem. Soc.* **1931**, 185.
(19) Moreland, C. G.; O'Brien, M. H.; Douthit, C. E.; Long, G. G. *Inorg. Chem.* **1968**, *7*, 834.
(20) Woods, C.; Long, G. G. *J. Mol. Spectrosc.* **1971**, *40*, 435.
(21) Bastiansen, O.; Graber, R.; Wegmann, L. *Balzers High Vac. Rep.* **1969**, *25*, 1.
(22) Ross, A. W.; Fink, M.; Hilderbrandt, R. *International Tables for Crystallography*; Wilson, A. J. C., Ed.; Kluwer Academic Publishers: Dordrecht, 1992; Vol. C, p 245.

Table 2. Electron Diffraction Measurements on $AsMe_5$ and $AsMe_3Cl_2$ Vapor: Details of the Data Sets[a]

	$AsMe_5$		$AsMe_3Cl_2$	
data set	I	II	I	II
camera dist, mm	497.0	247.1	498.9	249.0
nozzle temp, °C	25	26	92−101	92−100
sample temp, °C	−13	−5−0		
no. of plates	6	5	6	2
s-range, nm^{-1}	17.5−150.0	37.5−300.0	17.5−152.5	37.5−300.0
Δs, nm^{-1}	1.25	2.50	1.25	2.50
weight (*W*)	1.0	0.5	1.0	0.5

[a] The nozzle temperatures for $AsMe_3Cl_2$ are probably inaccurate because of an unfortunate placement of the thermocouples on the nozzle.

$AsMe_3Cl_2$ needed heating to give sufficient vapor pressure, and therefore the glass nozzle described above could not be used. A previous attempt to measure scattering patterns for this compound failed because of reactions with the metal surface of the nozzle. This time a heated ceramic nozzle was used, and no evidence of decomposition could be detected in the data. The plates were traced on an AGFA "Arcus II" scanner, and the results processed by a program written by Tor Strand.[24]

2.3. Molecular Mechanics Calculations. Molecular mechanics calculations on pentamethyl− and pentaphenyl−element compounds, EMe_5 and EPh_5, respectively, were carried out with the MM3 program of Allinger and co-workers.[25] The molecular energies were calculated as the sum of E−C bond stretching, ligand deformation, and ligand−ligand interaction energies.

E−C bonds were described by a Hill-like potential:

$$E_b(r) = \epsilon_b(1.84 \times 10^5\, e^{-12.0(r/r_b)} - 2.25(r_b/r)^6)$$

with $\epsilon_b = 209.2$ kJ mol^{-1}, and $r_b = 180$, 200, 222, or 230 pm, roughly corresponding to P−C, As−C, Sb−C, or Bi−C bond distances, respectively. This means that, within the formalism of the program, E−C bonds are treated as nonbonded interactions, and ∠CEC bending force constants need not be entered. Ligand deformation energies were calculated from standard expressions for bond stretching, angle bending, and torsional energies.[25] We have previously found that similar calculations reproduce the structural peculiarities of a number of metallocenes[26] and carboranes.[27]

The structures of TBP and SP models of EMe_5 were first optimized using a standard expression for van der Waals interactions between atoms in different ligands. The energy differences obtained, $E_{SP} - E_{TBP}$, are listed in the first column of Table 6. Since ab initio molecular orbital calculations[3] on $SbMe_5$ and $BiMe_5$ suggest that the metal atom carries a net positive (and the C atoms carry a net negative) charge, the calculations were repeated with the central atom carrying the charge +0.5, +1.5, or +2.5. The corresponding negative charge was distributed equally between the C atoms, which thus gained the charge −0.1, −0.3, or −0.5, respectively.

Experience has shown that, while molecular mechanics calculations on alkyl compounds reproduce experimental properties without the inclusion of C−H bond dipoles, such dipoles need to be taken into account for calculations on aromatic compounds. Calculations on EPh_5 were therefore carried out with the standard value for the C−H bond dipole, $\mu = 0.6$ D, and dipole−dipole and dipole−monopole interactions included in the ligand−ligand interaction energy.

3. Results

3.1. HF Computations. The primary aims of the HF calculations on $AsMe_5$ were to establish the ground-state symmetry of the molecule; to obtain a molecular force field for the calculation of root-mean-square vibrational amplitudes; and finally to estimate the energy difference between the TBP and SP configurations. For $AsMe_3Cl_2$ the questions of geometry are more readily answered by the GED results, and the calculations were performed for the sake of completeness. All calculations were performed with the program system Gaussian 94,[28] with the 6-31G* basis set.

The highest possible molecular symmetries for a TBP structure of $AsMe_5$ are C_{3h} and C_{3v}. A model of C_{3h} symmetry is shown in Figure 2; the equatorial methyl groups are oriented in such a manner that one C−H bond in each eclipses an adjacent equatorial As−C bond. A model of C_{3v} symmetry can be obtained by rotating all methyl groups 90° in a conrotatory manner to give a model in which one C−H bond from each equatorial methyl group eclipses one of the axial As−C bonds. The molecular symmetry C_{3h} implies perfect D_{3h} symmetry for the AsC_5 skeleton; the molecular symmetry C_{3v} does not. An SP structure can have C_{4v} skeletal symmetry, but the trigonal nature of the apical methyl group means that the highest possible molecular symmetry is C_s.

Optimization of C_{3h} and C_{3v} models yielded the lower energy for the former (see Table 3). The optimum structure parameters are listed in Table 4. The energy of the C_{3v} model is calculated, however, to be only 0.58 kJ mol^{-1} higher. An SP molecular model restricted to retain C_{4v} symmetry for the $C_{ap}As(C_{eq}H_3)_4$ fragment yielded an energy about 20 kJ mol^{-1} above the C_{3h} minimum. When this model was fully optimized under C_s symmetry, the coordination geometry collapsed to TBP.

The vibrational amplitudes of $AsMe_5$ were calculated from the C_{3h} force field using the program ASYM40;[29] the resulting amplitudes are listed in Table 4. The force field was scaled by a factor of 0.874, obtained by

(23) Andersen, B.; Seip, H. M.; Strand, T. G.; Stølevik, R. *Acta Chem. Scand.* **1969**, *23*, 3224.
(24) Gundersen, S.; Strand, T. G. *J. Appl. Crystallogr.* **1996**, *29*, 638.
(25) Allinger, N. L.; Yuh, Y. H.; Lii, J.-H. *J. Am. Chem. Soc.* **1989**, *111*, 8551.
(26) Timofeeva, T. V.; Lii, J.-H.; Allinger, N. L. *J. Am. Chem. Soc.* **1995**, *117*, 7452.
(27) Timofeeva, T. V.; Mazurek, U.; Allinger, N. L. *THEOCHEM* **1996**, *363*, 35.
(28) Frisch, M.J.; Trucks, G.W.; Schlegel, H.B.; Gill, P.M.W.; Johnson, B.G.; Robb, M.A.; Cheeseman, J.R.; Keith, T.; Petersson, G.A.; Montgomery, J.A.; Raghavachari, K.; Al-Laham, M.A.; Zakrzewski, V.G.; Ortiz, J.V.; Foresman, J. B.; Cioslowski, J.; Stefanov, B.B.; Nanayakkara, A.; Challacombe, M.; Peng, C.Y.; Ayala, P.Y.; Chen, W.; Wong, M.W.; Andres, J. L.; Replogle, E.S.; Gomperts, R.; Martin, R.L.; Fox, D.J.; Binkley, J.S.; Defrees, D.J.; Baker, J.; Stewart, J.P.; Head-Gordon, M.; Gonzalez, C.; Pople, J.A. Gaussian 94, Revision D.2; Gaussian, Inc.: Pittsburgh, PA, 1995.

Table 3. Results from Some HF Calculations on $AsMe_5$ and $AsMe_3Cl_2$[a]

symmetry	config	energy	imag freq
	$AsMe_5$		
C_{3h}	TBP	0.00	0
C_{3v}	TBP	0.58	1
C_s[b]	SP	19.55	3
C_s	SP → TBP	0.52	1
	$AsMe_3Cl_2$		
C_{3h}	TBP	1.19	3
C_{3v}	TBP	0.00	0

[a] Energies (in kJ mol^{-1}) relative to the most stable configuration. [b] $C_{ap}As(C_{eq}H_3)_4$ fragment restricted to C_{4v} symmetry.

Table 4. Results of the GED Analysis and HF Calculations for $AsMe_5$ on the Basis of a Trigonal Bipyramidal Model (C_{3h}). Distances (r_a) and Amplitudes Are in pm, Angles in Deg. Estimated Standard Deviations Are Given in Parentheses in Units of the Last Digit

parameter	GED[a]	HF[b]	GED/HF[c]
bond lengths			
As−C_{ax}	207.7(11)	206.7	207.3(4)
As−C_{eq}	197.4(6)	195.7	197.5(3)
C−H_{mean}	111.2(2)	108.4	111.2(2)
nonbonded distances			
C_{ax}···C_{eq}	286.5(5)	284.7	286.3(3)
C_{eq}···C_{eq}	341.9(11)	339.0	342.1(5)
C_{ax}···C_{ax}	415.3(21)	413.3	414.6(8)
As···H_{ax}	266.1(12)	265.4	265.8(9)
As···H_{eq}	256.7(15)	253.2	256.9(7)
amplitudes			
As−C_{ax}	7.5(15)	7.81	7.81[d]
As−C_{eq}	5.2(8)	5.47	5.47[d]
C−H_{mean}	10.2(3)	7.72	10.3(3)
C_{ax}···C_{eq}	9.3(5)	14.5	9.3(5)
C_{eq}···C_{eq}	23(8)	13.5	22(6)
C_{ax}···C_{ax}	11(7)	8.5	12(8)
As···H_{ax}	17(6)	14.5	17(5)
As···H_{eq}	12.3(17)	13.9	12(1)
valence angle			
∠AsCH_{mean}	109.4(8)	109.9	109.4(5)
R-factor[e]	3.21%		3.22%

[a] Results from GED analysis only. [b] Results from HF/ASYM40 calculations. [c] Results from GED analysis using As−C amplitudes calculated from the HF force field. [d] Fixed. [e] $R = \sqrt{\sum W(I_{obs}-I_{calc})^2/\sum I_{obs}{}^2}$.

comparing the four reported experimental frequencies[17,30] with the ab initio results.

$AsMe_3Cl_2$ was optimized on the C_{3h} model shown in Figure 2 and on a C_{3v} model with C−H bonds eclipsing one of the axial As−Cl bonds. Somewhat surprisingly, slightly lower energy was obtained for the C_{3v} conformation, as shown in Table 3. The structural parameters from the C_{3h} computation are listed in Table 5. As the standard deviations for the experimental parameters are acceptable, we have not found it necessary to compute the vibrational amplitudes for this molecule.

3.2. Structure Refinements. 3.2.1. $AsMe_5$. Structure refinements were based on a molecular model of C_{3h} symmetry (see Figure 2). All methyl groups were assumed to have local C_{3v} symmetry and to be equidimensional. Axial methyl groups were fixed in a staggered orientation with respect to the equatorial AsC_3 unit, as indicated by the HF calculations. The structure

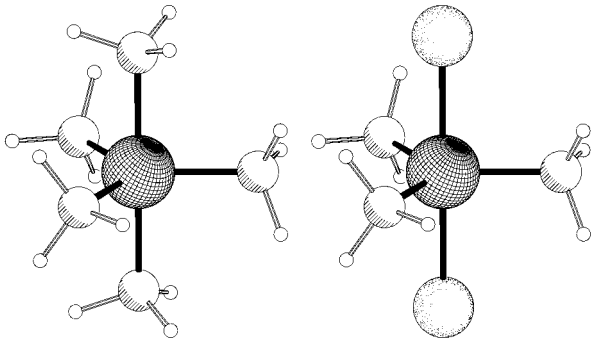

Figure 2. Molecular models for pentamethylarsenic(V) (left) and trimethyldichloroarsenic(V) (right).

Table 5. Results of the GED Analysis and HF Calculations for $AsMe_3Cl_2$ on the Basis of a Trigonal Bipyramidal Model (C_{3h}). Distances (r_a) and Amplitudes Are in pm, Angles in deg. Estimated Standard Deviations Are Given in Parentheses in Units of the Last Digit

parameter	GED[a]	HF[b]
bond lengths		
As−Cl	234.9(3)	237.6
As−C	192.5(2)	192.6
C−H_{mean}	109.9(5)	107.9
nonbonded distances		
Cl···C	303.7(4)	305.8
C···C	333.5(4)	333.5
Cl···Cl	469.8(6)	475.1
amplitudes		
As−Cl	7.7(2)	
As−C	5.4(4)	
C−H_{mean}	8.4(7)	
Cl···C	10.7(3)	
C···C	19.3(32)	
Cl···Cl	8.2(7)	
valence angle		
∠AsCH_{mean}	109.5(8)	108.0
R-factor[c]	5.00%	

[a] Results from GED analysis. [b] Results from HF calculations. Amplitudes not computed. [c] $R = \sqrt{\sum W(I_{obs}-I_{calc})^2/\sum I_{obs}{}^2}$.

is then defined by four independent parameters, *r*(As−C_{ax}), *r*(As−C_{eq}), *r*(C−H)$_{mean}$, and ∠AsCH, all of which yielded to independent refinement. The main results from the refinement are given in Table 4. In addition, 17 vibrational amplitudes could be refined; although all the nonbonded C···H amplitudes and the mean H···H amplitude for two hydrogen atoms of the same methyl group were refined, they had no significant effect on the structure and so have been omitted from Table 4.

The standard deviations for the As−C bond lengths derived from the refinement of the GED data alone were unsatisfactorily large, up to 1.1 pm. Since fixing an amplitude usually decreases the standard deviation of the corresponding distance, we have appealed to the ab initio computations on $AsMe_5$ for estimates of the vibrational amplitudes for the As−C bonds based on the calculated molecular force field. Refinements with the amplitudes fixed at the calculated values yielded the results given in the last column in Table 4. Figures 3 and 4 show the modified molecular intensity and the radial distribution curves, respectively, as afforded by the GED analysis.

An SP model was also tested in the GED refinements, but the high *R*-factor (21%) made it clear that the data were not compatible with this geometry. Moreover, the

(29) Hedberg, L.; Mills, I. M. *J. Mol. Spectrosc.* **1993**, *160*, 117.
(30) Eberwein, B.; Ott, R.; Weidlein, J. *Z. Anorg. Allg. Chem.* **1977**, *431*, 95.

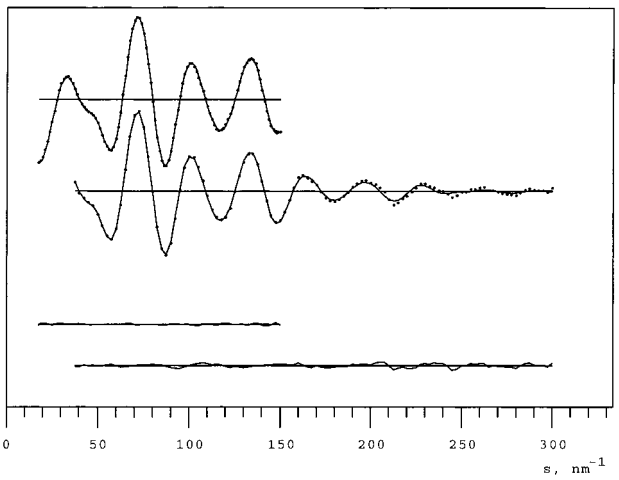

Figure 3. Calculated (full line) and experimental (dots) modified molecular intensity curves for $AsMe_5$ with difference curves below.

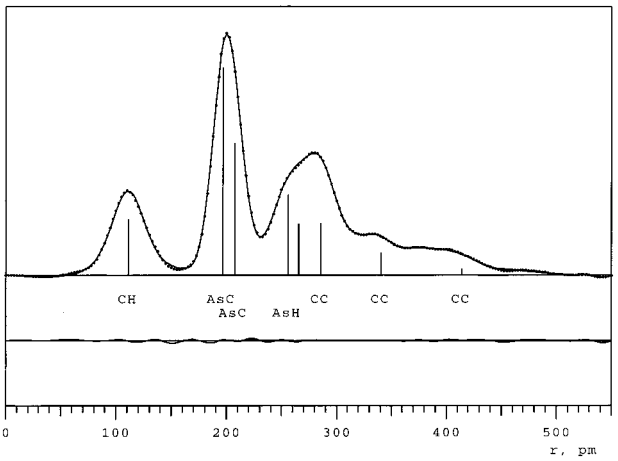

Figure 4. Calculated (full line) and experimental (dots) radial distribution curves for $AsMe_5$. The artificial damping constant was $k = 25$ pm^2. The most important peaks are indicated by bars each with a height approximately equal to the weight of the distance in the calculated intensity curve. The difference curve is shown below.

radial distribution for this refinement showed severe misfit in the region of the C···C distances.

3.2.2. $AsMe_3Cl_2$. Structure refinements for this molecule were based on a model of C_{3h} symmetry, as shown in Figure 2. The same restrictions were imposed on the methyl groups as with $AsMe_5$; that is, they were assumed to have local C_{3v} symmetry and were fixed so that one C−H bond is situated in the equatorial plane. The structure is defined by four independent parameters, $r(As-Cl_{ax})$, $r(As-C_{eq})$, $r(C-H)_{mean}$, and ∠AsCH, all of which yielded to independent refinement. The main results from the refinement are given in Table 5; other nonbonded vibrational amplitudes could be refined, but are not tabulated. The molecular intensity and the radial distribution curves are given in Figures 5 and 6, respectively.

As the ab initio calculations suggested the C_{3v} conformer to be more stable, we also refined such a model to the GED data. The fit was, however, not as good as for the C_{3h} model; the *R*-factor could not be brought below 6% while still retaining reasonable amplitudes. Also, the radial distribution curves for this refinement

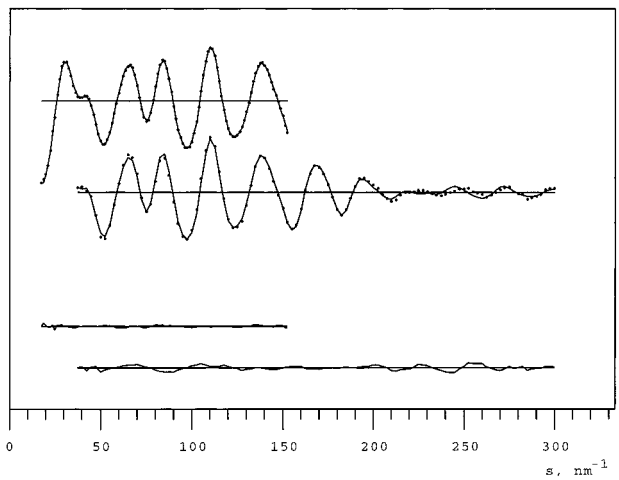

Figure 5. Calculated (full line) and experimental (dots) modified molecular intensity curves for $AsMe_3Cl_2$ with difference curves below.

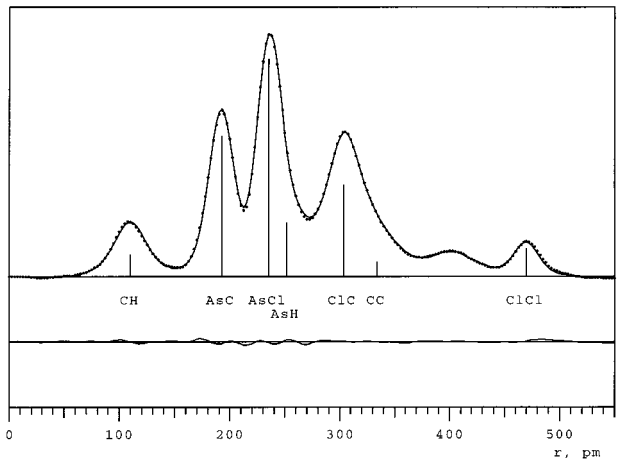

Figure 6. Calculated (full line) and experimental (dots) radial distribution curves for $AsMe_3Cl_2$. The artificial damping constant was $k = 25$ pm^2. The difference curve is shown below.

showed some misfit in the region of the peak at 400 pm which contains the larger Cl···H and C···H distances.

4. Discussion

4.1. The Structure of $AsMe_5$. The fit between the experimental GED data and those calculated for an SP model of $AsMe_5$ is so poor that such a model can be ruled out with confidence. A TBP model of C_{3h} symmetry (Figure 2), on the other hand, is in excellent agreement with the GED data. We deduce that the AsC_5 frame has D_{3h}, or near-D_{3h}, symmetry. This conclusion is in accord with the results of the HF calculations, which indicate that the energy of the SP configuration is about 20 kJ mol^{-1} above that of the TBP configuration, and also with the inferences drawn from the infrared and Raman spectra of the liquid.[17,30]

As seen from Table 4, the bond distances derived from the HF calculations are in good agreement with the GED values. The fixing of the amplitudes in the GED refinement causes no significant change in the structural parameters, but reduces the standard deviations. The structural parameters thus determined must be considered to be to the best possible on the basis of the data currently available.

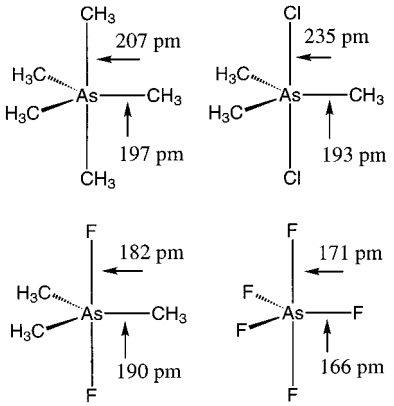

Figure 7. Structural parameters of gaseous $AsMe_5$ and $AsMe_3Cl_2$ (this work), $AsMe_3F_2$,[34] and AsF_5.[35]

In $AsMe_3$[31] the As−C bond distance is 196.8(3) pm, virtually identical to the r(As−C_{eq}) found for $AsMe_5$ in this study. In $SbMe_5$[2] the skeletal distances are r_{ax} = 226.4(11) pm and r_{eq} = 214.0(5) pm. As the covalent radius for Sb is ca. 20 pm greater than for As (141 pm vs 120 pm[32]), the bond lengths found for $AsMe_5$ are quite consistent with those of $SbMe_5$.

4.2. The Structure of $AsMe_3Cl_2$. The GED data are in excellent agreement with a molecular model of C_{3h} symmetry, as shown in Figure 2. Both the TBP coordination geometry and the axial positions of the Cl atoms receive unequivocal confirmation from the distinct peak in the radial distribution curve corresponding to the distance between two Cl atoms spanning a linear ClAsCl unit (see Figure 6).

The C_{3v} conformer gave a poorer fit, but cannot be ruled out. The HF calculations indicate a barrier to internal rotation of the methyl groups of only about 1.2 kJ mol^{-1}. This barrier is lower than the thermal energy at room temperature ($RT \approx 2.5$ kJ mol^{-1}) and indicates that the methyl groups will undergo virtually nonhindered rotation. We have chosen to report here only the results from the C_{3h} refinement and calculation.

An investigation by single-crystal X-ray diffraction shows that the gas-phase configuration is retained in the solid state,[33] and the As−C_{eq} bond distance, 193(2) pm, is in good agreement with the GED value. At 245(4) pm the As−Cl_{ax} bond distance in the solid is 11 pm longer than the corresponding distance in the gaseous molecule, but the large estimated standard deviation of the former makes the difference of uncertain statistical significance.

Up to the present time only four pentavalent compounds of arsenic have been characterized structurally in the gas phase, viz., $AsMe_5$, $AsMe_3Cl_2$ (this work), $AsMe_3F_2$,[34] and AsF_5[35] (see Figure 7). The thermal frailty of $AsCl_5$, which decomposes at temperatures above −50 °C,[36] precludes the structural characterization of the gaseous molecule. All compounds are TBP, and in the mixed compounds the more electronegative substituents occupy the axial positions. It is seen that introduction of two Cl atoms in the axial positions of $AsMe_5$ reduces the equatorial As−C bond distances from 196.7(3) to 192.5(2) pm and that replacement of the Cl atoms by the more electronegative F atoms leads to a further reduction of these distances to 189.7(6) pm. Finally, replacement of the three equatorial methyl groups in $AsMe_3F_2$ by F atoms reduces the axial As−F distance from 182.0(6) pm to 171.1(5) pm. It appears therefore that axial bond distances are more sensitive to inductive effects than are equatorial ones. As a result, the difference between axial and equatorial bond distances is only half as large in AsF_5 as in $AsMe_5$.

Table 6. Energy Difference (in kJ mol^{-1}) between Square Pyramidal (SP) and Trigonal Bipyramidal (TBP) Configurations of EMe_5 and EPh_5 Compounds, $E_{SP} - E_{TBP}$, As Calculated by Molecular Mechanics (MM3) as a Function of the Charge on Each C_α Atom, q_C, and the E−C Bond Distance

	q_C			
E−C	0.0	−0.1	−0.3	−0.5
		EMe_5		
180 pm	1.9	2.2	3.4	5.6
200 pm	1.0	1.1	1.9	3.3
222 pm	0.3	0.4	2.2	2.1
230 pm	0.1	0.3	1.0	1.8
		EPh_5		
180 pm	20.0	8.2	8.5	10.7
200 pm	3.5	2.6	1.6	2.1
222 pm	−0.3	−1.3	−2.7	−3.6
230 pm	−1.0	−2.1	−3.7	−4.1

4.3. Coordination Geometries and Ligand−Ligand Interaction Energies Estimated by Molecular Mechanics Calculations. Structure optimization of EMe_5 without charges on E or C atoms yields energy differences between optimized models, $E_{SP} - E_{TBP}$, ranging from 1.9 to 0.1 kJ mol^{-1} when the E−C bond distance (r_b) is increased from 180 to 230 pm (see Table 6). Assignment of net negative charges to the C atoms leads to further relative destabilization of the SP geometry, particularly if the E−C bond distance is short or the net charge on C is large.

The calculations thus indicate that ligand−ligand interactions in these compounds stabilize the observed TBP coordination geometry. The relative energy of the SP coordination geometry is, however, lower than that estimated by ab initio calculations, presumably because the latter include electronic effects which also stabilize the TBP geometry.

Structure optimization of EPh_5 without E−C or C−H bond dipoles yields energy differences between optimized SP and TBP models which range from 23.7 to 1.5 kJ mol^{-1} when E−C is increased from 180 to 230 pm (the results are not tabulated). As for the pentamethyl compounds, van der Waals forces between the ligands tend to stabilize the TBP relative to the SP model. Experience has shown, however, that it is necessary to include C−H bond dipoles to secure agreement between calculated and experimental properties of aryl compounds.[25] Inclusion of such dipoles leads to *inversion* of the relative energies of the SP and TBP models for the longer E−C bonds (see Table 6). Inclusion of M−C dipoles leads to a further relative stabilization of the SP model. It would thus appear that ligand−ligand

(31) Blom, R.; Haaland, A.; Seip, R. *Acta Chem. Scand.* **1983**, *A37*, 595.
(32) Blom, R.; Haaland, A. *J. Mol. Struct.* **1985**, *128*, 21.
(33) Hursthouse, M. B.; Steer, I. A. *J. Organomet. Chem.* **1971**, *27*, C11.
(34) Downs, A. J.; Goode, M. J.; McGrady, G. S.; Steer, I. A.; Rankin, D. W. H.; Robertson, H. E. *J. Chem. Soc., Dalton Trans.* **1988**, 451.
(35) Clippard, F. B., Jr.; Bartell, L. S. *Inorg. Chem.* **1970**, *9*, 805.
(36) Seppelt, K. *Angew. Chem., Int. Ed. Engl.* **1976**, *15*, 377.

interactions contribute to the stabilization of the observed SP coordination geometries of $SbPh_5$ and $BiPh_5$.

Acknowledgment. We are grateful to the VISTA program of STATOIL and the Norwegian Academy of Science and Letters for financial support and to the Norwegian Research Council (Program for Supercomputing) for a grant of computer time; to the EPSRC for financial support and for an Advanced Fellowship (to T.M.G.); to the Royal Society for a Research Fellowship (to C.R.P.); and to CRDF Grant RC2-147 (to T.V.T). Further, we are grateful to Dr. Ole Swang and an anonymous referee for useful advice concerning ab initio calculations.

OM980520R